Available online at www.sciencedirect.com
SCIENCE DIRECT®
Journal of Sound and Vibration 290 (2006) 1119–1140
JOURNAL OF SOUND AND VIBRATION
www.elsevier.com/locate/jsvi

Effects of disorder in one- and two-dimensional micromechanical resonator arrays for filtering

John A. Judge[a,*], Brian H. Houston[b], Douglas M. Photiadis[b], Peter C. Herdic[c]

[a]*Mechanical Engineering Department, The Catholic University of America, Washington, DC 20064, USA*
[b]*Code 7130, Naval Research Laboratory, Washington, DC 20375, USA*
[c]*SFA, Inc., Largo, MD 20774, USA*

Received 7 June 2004; received in revised form 2 May 2005; accepted 7 May 2005
Available online 25 July 2005

Abstract

The effects of disorder on the vibration behavior of arrays of micromechanical resonators are investigated, and the consequences for the characteristics of filters comprised of such arrays are described. Existing understanding of the phenomenon of localization is applied to demonstrate that such devices are particularly sensitive to small variations among resonators which are nominally identical, and that, in the case of high-Q resonators, disorder-induced vibration localization can be a significant impediment to improving filter performance. Numerical simulations are employed to demonstrate the typical effects of different levels of disorder. A novel two-dimensional array of resonators is proposed that is less sensitive to disorder than conventional one-dimensional arrays, improving filter performance without the need for improved manufacturing tolerances.

1. Introduction

Bandpass filters in the RF and IF stages of modern communication systems are typically implemented as vibrating mechanical tank components, such as crystal and SAW resonators. These devices dramatically outperform filters implemented using transistor technologies. However, they are off-chip components, with significant size that is an obstacle to further

*Corresponding author. Tel.: 202 319 5127; fax: 202 319 5173.
E-mail address: judge@cua.edu (J.A. Judge).

0022-460X/$ - see front matter © 2005 Elsevier Ltd. All rights reserved.
doi:10.1016/j.jsv.2005.05.003

miniaturization of wireless transceivers. One path to overcoming this obstacle is to use microscale mechanical resonators manufactured directly on-chip [1–8]. Arrays of these resonators, which can have quality factors over 500,000 [9], can be used to construct filters with low insertion loss in the passband and excellent shape factor and rejection outside the passband. To date, two-resonator and three-resonator prototypes of such filters have been demonstrated [5–8]. In the case of one-dimensional (1-D) arrays, the number of resonators is synonymous with the order of the filter. Arrays with larger numbers of resonators can thus, in theory, provide sharper rolloffs and higher stopband rejection. However, successful implementation of such filters is complicated by increased susceptibility to passband-distorting mismatches between resonators.

A chain of multiple identical mechanical resonators is a spatially periodic system, and the behavior of such systems has been well understood for decades [10,11]. In frequency passbands, energy-carrying waves can propagate freely along the chain without attenuation, whereas at frequencies outside the passbands, wave amplitudes decay exponentially along the chain. In practice, the periodicity of such a chain is destroyed by mismatches between resonators, caused by inevitably imperfect manufacturing tolerances. This deviation from periodicity causes partial reflections of the energy-carrying waves traveling from resonator to resonator, leading to spatial decay of amplitude even at frequencies within the passbands. The propagation of vibration energy in such systems is analogous to the diffusion of electrons in disordered lattices, for which the phenomenon of spatial attenuation due to aperiodicity was first explained by Anderson [12]: it has since become known as Anderson localization. The first person to apply Anderson's findings to mechanical systems was Hodges [13], who showed that the degree of localization depends on the ratio of the strength of the disorder to the strength of the coupling between subsystems, i.e., weakly coupled arrays are more susceptible to localization for a given amount of periodicity-breaking disorder. The effect of disorder on mechanical vibration has since been studied in a wide variety of nominally periodic macroscale structures, including multi-span beams and multi-bay trusses [14–18], periodically ribbed cylinders [19,20], ribbed antennas [21], and cyclically symmetric structures such as turbomachinery stages [22,23].

Localization due to aperiodicity can pose a significant problem for the use of arrays of micromechanical resonators as filters. Since the width of the passband of a nominally periodic resonator array is a function of the coupling between resonators, implementing the narrow bandpass filters typically required by communication devices necessitates weak coupling, making such arrays particularly prone to localization when disorder is present. In an array of perfectly identical resonators, dissipation due to damping is the only source of spatial attenuation of energy in the passband; the insertion loss of a bandpass filter implemented using such resonators would depend only on the number of resonators and the resonator quality factor, or Q. In reality, however, the resonators can never be perfectly identical, and localization effects due to resonator variation can cause significant passband distortion, degrading the performance of the filter. Moreover, as resonators with increasingly high Q's are developed, minimizing losses due to damping, spatial attenuation due to localization becomes the dominant cause of insertion loss. Castanier and Pierre [24] present an analysis of the combined effects of dissipation and disorder-induced localization on energy transmission along a 1-D chain of oscillators, using perturbation methods to find approximate expressions for the spatial decay rate in the limits of strong and weak inter-oscillator coupling.

The effect of localization on filter performance can be reduced by decreasing the amount of disorder in the system, either by improving manufacturing tolerances so that the resonators are

more nearly identical, or by post-fabrication adjustment of the resonators. This "tuning" has been accomplished by Nguyen et al. [2] (see also Refs. [6–8]), who electrically compensated for variations by adjusting the resonant frequencies of the individual resonators using DC-bias voltages applied to each resonator. An effective electrical spring stiffness, which depends on the bias voltage, modifies the mechanical spring stiffness of each resonator: the applied voltages are iteratively adjusted until all resonant frequencies are matched and the desired passband, free of the effects of disorder, is achieved. Although such a technique is well applied to prototypes, the added cost associated with individually tuning each filter makes it inappropriate for the eventual mass production of such devices. Given the difficulty in reducing the amount of disorder in an array, especially in any cost-effective way, there is a strong need to develop designs that have reduced sensitivity to disorder.

The purpose of this paper is to investigate the effects of disorder on the behavior of micromechanical resonator arrays, allowing the design of arrays with reduced sensitivity to disorder. In Section 2, existing understanding of localization is applied to 1-D arrays of microscale resonators, allowing designers of such structures to determine the degree to which disorder is a problem for a given design. In Section 3, the results of numerical simulations of disordered 1-D arrays of single degree of freedom oscillators are shown, providing examples of the effects described in Section 2. Finally, in Section 4, a two-dimensional (2-D) array is proposed that can be used to reduce sensitivity to disorder by acting as a 1-D chain with reduced levels of disorder.

2. Spatial attenuation of vibration amplitude in microscale resonator arrays

2.1. Wave propagation in a 1-D array of identical oscillators

Consider a simple model of a chain of identical resonators, in which each resonator is represented by a single degree of freedom oscillator (see Fig. 1). Each oscillator has the same mass, m, and nominal stiffness, k_0, and adjacent oscillators are coupled by a stiffness k_c. If the non-dimensional coupling is defined as $R = k_c/k_0$, and the natural frequency of an individual oscillator is $\omega_0 = \sqrt{k_0/m}$, then the passband of the system will consist of frequencies between ω_0 and $\omega_0\sqrt{1+4R}$. This can be shown by considering the equation of motion of a single oscillator,

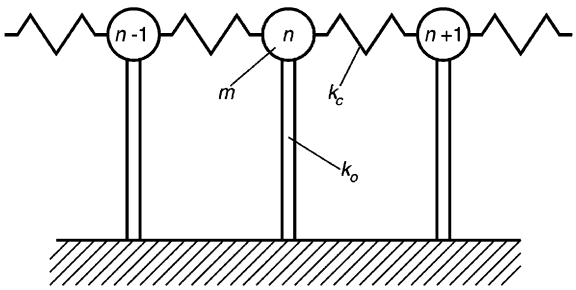

Fig. 1. Single degree of freedom model of 1-D oscillator chain. Each oscillator has the same mass, m, and nominal stiffness, k_0. Adjacent oscillators are coupled by stiffness k_c.

coupled to its neighbor on either side:

$$-\omega^2 m u_n + (k_0 + 2k_c)u_n - k_c u_{n-1} - k_c u_n + 1 = 0. \tag{1}$$

Here, u_n is the vibration amplitude of oscillator n, and u_{n-1} and u_{n+1} are the amplitudes of the neighbors to left and right, respectively.

Following the transfer matrix approach used by Castanier and Pierre [24], this equation can be rewritten, after dividing through by k_c and substituting $k_c/k_0 = R$, as

$$\begin{Bmatrix} u_{n+1} \\ u_n \end{Bmatrix} = T \begin{Bmatrix} u_n \\ u_{n-1} \end{Bmatrix}, \quad T = \begin{bmatrix} \left(\frac{1+2R-\omega^2/\omega_0^2}{R}\right) & -1 \\ 1 & 0 \end{bmatrix}. \tag{2}$$

The eigenvalues of T are simply

$$\lambda_{1,2} = \tfrac{1}{2}(T_{1,1} \pm \sqrt{T_{1,1}^2 - 4}). \tag{3}$$

If $T_{1,1}^2 < 4$, which is the case if ω/ω_0 is between 1 and $\sqrt{1+4R}$, both eigenvalues will be complex and have magnitude 1. If ω/ω_0 is outside that range, $T_{1,1}^2$ will be greater than 4, so both eigenvalues will be real: λ_1 will be greater than one, and λ_2 will be its reciprocal. The matrix of eigenvectors corresponding to λ_1 and λ_2 can be used to transform T into a wave transfer matrix, W_0

$$\begin{Bmatrix} \mathsf{L}_{n+1} \\ \mathsf{R}_{n+1} \end{Bmatrix} = W_0 \begin{Bmatrix} \mathsf{L}_n \\ \mathsf{R}_n \end{Bmatrix}, \quad W_0 = \begin{bmatrix} \lambda_1 & 0 \\ 0 & \lambda_2 \end{bmatrix} \tag{4}$$

relating the amplitudes of left- and right-going waves (L and R) on either side of oscillator n. If both eigenvalues have magnitude 1, waves can undergo a phase shift but do not change amplitude as they pass the oscillator; however, outside $\omega_0 < \omega < \omega_0\sqrt{1+4R}$, the eigenvalues have magnitude other than 1, and the matrix W_0 determines the attenuation of the waves as they pass the oscillator. Since a wave's amplitude is reduced by the same fraction ($|\lambda_2|$, or $1/|\lambda_1|$) as it crosses each oscillator, the spatial amplitude decay is exponential, with the rate of exponential decay per oscillator defined as

$$\gamma = \ln |\lambda_1|. \tag{5}$$

The same result can be achieved by rewriting Eq. (1) as

$$a_2 \nabla^{(2)} u = [(\omega^2 m - k_0)/k_c]u \tag{6}$$

and noting the similarity to the 1-D wave equation, $\nabla^2 u = (\omega^2/v^2)u$. Eq. (6) is nearly identical to the equation given by Sheng [25] for waves on a discrete lattice, but with the additional effect of each oscillator's inherent stiffness, k_0. Here, $\nabla^{(2)}$ indicates a discrete form of the Laplacian (∇^2, or $\partial^2/\partial x^2$ in 1-D) equal to $1/a^2(u_{n-1} + u_{n+1} - 2u_n)$, and a is the spacing between oscillators. Since a is the minimum length scale of the system, there cannot be a wave traveling through the chain of oscillators with wavelength less than $2a$: the maximum wavenumber k is thus π/a. Mathematically, this is expressed by the fact that, unlike the continuous Laplacian, for which any wavenumber k is an eigenvalue, the eigenvalues of the 1-D discrete Laplacian are given by $e(k) = 2/a^2(1 - \cos ka)$ [25], found by substituting $u_n = \exp(-i\omega t)$, $u_{n-1} = \exp(-i\omega t - ika)$, and $u_{n+1} = \exp(-i\omega t + ika)$ into $\nabla^{(2)}$. Wavenumbers greater than π/a are therefore indistinguishable from lower wavenumbers, and all eigenvalues $e(k)$ are between 0 and $4/a^2$, corresponding to wavenumbers between 0 and π/a.

Replacing $\nabla^{(2)}u$ with $e(k)u$ in Eq. (6) and solving for ω^2 gives

$$\omega^2 = \frac{k_0 + k_c a^2 e(k)}{m} = \omega_0^2(1 + 2(1 - \cos ka)R). \tag{7}$$

The frequencies at which waves propagate through the system are thus between $\omega = \sqrt{k_0/m}$ (corresponding to wavenumber $k = 0$) and $\omega = \sqrt{(k_0 + 4k_c)/m}$ (corresponding to wavenumber π/a), i.e., frequencies between ω_0 and $\omega_0\sqrt{1 + 4R}$.

Note that the width of the passband, which is approximately $2R\omega_0$ for small R, depends only on the nominal oscillator frequency and the amount of coupling. For weakly coupled systems, the percent bandwidth is thus simply twice the non-dimensional coupling, regardless of the number of oscillators in the chain. Filters for RF and IF applications typically have bandwidths between a few tenths of 1% and a few percent of the filter center frequency. In order to use a chain of resonators to implement such a filter, the coupling ratio R must indeed be small—this can be accomplished by designing an array in which the coupling stiffness is significantly softer than the stiffness of the resonators themselves. Although fabrication considerations place a lower limit on the thickness and width (and thus stiffness) of beams used to mechanical couple adjacent resonators, the coupling stiffness can also be decreased by attaching the coupling beams to the resonators far away from the location of maximum vibration amplitude [3,6–8], allowing small R to be achieved using coupling beam with reasonable dimensions. Note that the ratio of filter center frequency to filter bandwidth is often referred to as the filter quality factor, Q_{filter}, and is equal to $1/2R$ for small R. This should not be confused with the individual resonator quality factor, Q, which is determined by the amount of damping present in the resonant mode of a single device.

2.2. Spatial decay due to damping

The addition of damping to an array of identical oscillators adds an imaginary term to the oscillator equation of motion, Eq. (1), proportional to the damping coefficient δ (the reciprocal of the oscillator quality factor, Q). This adds a factor $j\delta/R$ to the (1,1) term of the displacement transfer matrix T (where $j = \sqrt{-1}$). The eigenvalues of T no longer have unit magnitude within the passband, and thus the spatial decay constant γ is non-zero at all frequencies. If the damping δ is small compared to coupling R, the damped spatial decay constant within the passband is shown by Castanier and Pierre [24] to be

$$\gamma_d \approx \frac{1}{\sqrt{\alpha(4 - \alpha)}}\left(\frac{\delta}{R}\right), \tag{8}$$

where the passband position, α, is defined by $(\omega/\omega_0)^2 = 1 + \alpha R$, so that $0 \leqslant \alpha \leqslant 4$ within the passband.

Energy dissipation mechanisms in micromechanical resonators have been the subject of much recent investigation [26–31]. Significant sources of dissipation can include acoustic and viscous losses (if the oscillator is in a fluid such as air), intrinsic absorption within the material (phonon–phonon interaction and thermoelastic dissipation), and losses through the attachment of the resonator to the supporting structure. Typically, high-Q resonators are operated in vacuum, eliminating acoustic and viscous losses, while intrinsic material loss and attachment loss are small enough that Q's on the order of 10^3–10^5 [30,32–34], and in some cases over 5,00,000 [9], can be

achieved. For an application with a narrow bandwidth requirement of 0.1% ($Q_{\text{filter}} = 1000$, or $R \approx 0.005$) and resonator Q of 10,000 ($\delta = 10^{-4}$) the spatial decay constant γ_d is less than 0.1 at passband center, indicating less than 0.5 dB transmission loss per resonator. Thus, if damping were the only significant source of energy attenuation across the length of the chain, low-loss filters could be achieved using chains significantly longer than the existing two- and three-resonator prototypes.

2.3. Localization due to disorder

Wave amplitudes can also decay in the passband in an undamped system, if the resonators are not precisely identical. Resonators may have slightly different dimensions, due to manufacturing tolerances, and may have other variability due to material defects, surface roughness, etc. Here, all such causes of disorder are modeled as variations in oscillator stiffness. Depending on the mechanism used to couple adjacent oscillators, the coupling stiffness may also vary throughout the array; however, such effects are neglected here. If the stiffness k_n of oscillator n varies from the nominal oscillator stiffness, k_0, by a fractional amount Δk_n (defined as $(k_n - k_0)/k_0$), then an additional $\Delta k_n/R$ will be added to the (1,1) term of the displacement transfer matrix, T, for oscillator n. If the eigenvalues of the nominal T matrix are used to transform the modified T matrix for oscillator n, the resulting wave transfer matrix, W_n, will have off-diagonal terms. W_n can be written as

$$W_n = \begin{bmatrix} 1/t_n & -(r_n/t_n) \\ r_n/t_n & t_n - (r_n^2/t_n) \end{bmatrix}, \tag{9}$$

where t_n is a transmission coefficient and r_n is a reflection coefficient. Without disorder, the transmission coefficient, t_n, is simply the eigenvalue λ_2 (the reciprocal of λ_1), which has magnitude 1 within the passband, and the reflection coefficient, r_n, is zero. In the presence of disorder, however, the transmission and reflection coefficients become

$$t_n = \frac{\lambda_2}{(1+\beta)}, \quad r_n = \frac{-\lambda_2 \beta}{(1+\beta)}, \tag{10}$$

where β is $\Delta k_n/(R(\lambda_1 - \lambda_2))$. As the difference in stiffness between oscillator n and the nominal oscillator increases, a greater percentage of the energy in an incident wave is reflected rather than transmitted. As the wave propagates across multiple oscillators, the total transmission and reflection can be found by calculating the global wave transfer matrix, $\mathscr{W}$, which is the product of each oscillator's wave transfer matrix W_n. The transmission, t_n, at each oscillator depends on the individual oscillator stiffness, and thus spatial decay of amplitude along the chain is not smooth. However, in the limit as $N \to \infty$, the spatial amplitude decay is asymptotically exponential, and the (1,1) element of the global matrix $\mathscr{W}$ can be used to find an average rate of decay per oscillator:

$$\gamma = \lim_{N \to \infty} \frac{1}{N} \ln |\mathscr{W}_{(1,1)}|. \tag{11}$$

In this case, γ can be called a *localization factor*, and is essentially the reciprocal of the decay length, ξ, defined by Sheng [25] for localization in a 1-D array, normalized by the spacing between

oscillators. In general, the differences between resonators in any array may include some systematic variation as well as random, uncontrollable variations; it is the latter that are modeled here, allowing overall disorder in the system to be characterized by σ, the standard deviation of the variations in stiffness, Δk_n. Without disorder, $\mathscr{W}_{(1,1)}$ has magnitude 1 within the passband; as σ increases, the magnitude of $\mathscr{W}_{(1,1)}$ decreases, and the increased spatial decay of amplitude reflects greater localization of energy near the beginning of the chain. Note that, if disorder were modeled as a variation in some other parameter than oscillator stiffness (mass, for example), the details of the calculation of t_n and r_n (and thus $\mathscr{W}$) would be slightly different, but the qualitative effect would be the same.

2.4. Combined effects of disorder and dissipation

Castanier and Pierre [24] present expressions, based on perturbation analysis, for the (average) exponential decay constant for a system with both damping and disorder, called the *damped localization factor*, γ_{md}. For systems in which both the ratio of dissipation to coupling, δ/R, and the ratio of disorder to coupling, σ/R, are small, classical perturbation techniques can be used; if either of these ratios is large, a modified perturbation technique must be used, in which coupling is considered the disturbance. Since a high-performance filter requires minimal spatial attenuation across the chain, low levels of both damping and disorder are highly desirable, and thus only the former case is considered here. Although Castanier and Pierre refer to this as the *strong-coupling approximation*, it is valid as long as coupling, R, is strong compared to damping, δ, and disorder, σ, i.e., coupling can be quite small as long as damping and disorder are smaller still. Within the passband, the damped localization factor (based on the strong-coupling approximation) is

$$\gamma_{md} \approx \frac{1}{\sqrt{\alpha(4-\alpha)}}\left(\frac{\delta}{R}\right) + \frac{1}{2\alpha(4-\alpha)}\left(\frac{\sigma}{R}\right)^2 \tag{12}$$

which, at the passband center ($\alpha = 2$), reduces to

$$\gamma_{md} \approx 1/2(\delta/R) + 1/8(\sigma/R)^2. \tag{13}$$

Thus, disorder becomes a significant source of spatial decay if $(\sigma/R)^2$ is non-negligible, and the dominant source of decay if $(\sigma/R)^2$ is large relative to (δ/R). Fig. 2 shows the damped localization factor, γ_{md}, at the passband center, versus normalized disorder, σ/R, for various amounts of damping, based on the above approximation. If the percentage variation among oscillators approaches or exceeds the coupling (half the percent bandwidth), then the strong-coupling approximation breaks down, however, by this point, the spatial decay due to disorder is already too large to be adequate for use in a low-insertion loss filter. The limits of fabrication tolerances set a lower limit on the percentage bandwidth achievable without significant passband distortion and insertion loss, regardless of the extent to which dissipation is minimized. Clearly, improving the Q of microscale resonators is of no benefit for filtering applications unless disorder-induced localization can also be avoided, either by improved fabrication precision, post-fabrication "tuning" of resonators, or by design of microscale resonator filters that are less sensitive to disorder than simple 1-D chains.

It is important to note that γ_{md} is an average quantity, which gives an accurate measure of the decay-per-oscillator only in the limit of large numbers of oscillators. Nevertheless, for smaller

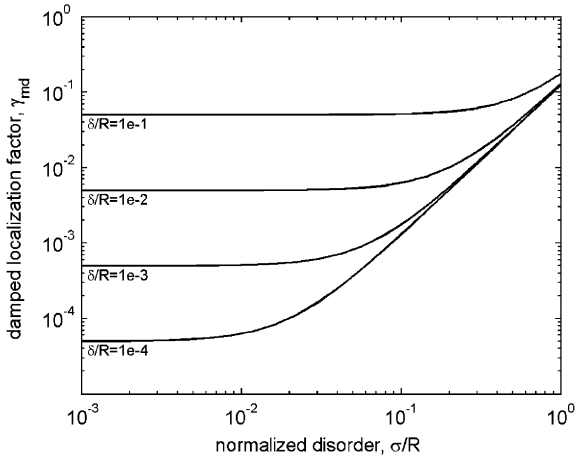

Fig. 2. Damped localization factor (exponential decay constant) at passband center as a function of normalized disorder, for various levels of damping.

numbers of oscillators, examination of γ_{md} provides insight into the relative effects of damping and disorder, even though it cannot be used to accurately predict the signal amplitude at the end of the chain.

3. Simulation of 1-D oscillator chains as filters

The global wave transfer matrix $\mathscr{W}$, and thus the attenuation of a signal traveling through an oscillator chain, can only be evaluated in a statistical sense, in the limit of large N, unless the specific variation of each oscillator is known. In general, resonator variations are random, and have magnitude dictated by manufacturing tolerances. Although examination of the average spatial attenuation is useful for gaining an understanding of the levels of disorder required to cause non-negligible effects, the effects themselves are more easily understood by examining the exact transmission characteristics of specific, randomly disordered cases, using numerical simulations. In this section, the results of such simulations are presented, demonstrating the effects of disorder on the transmission spectra of 1-D oscillator chains. Note that the results shown here are based on simulations of the full dynamics of specific coupled oscillator chains, and thus do not depend on the strong-coupling approximation made in Eqs. (12) and (13) which allowed γ_{md} to be evaluated statistically.

3.1. Transmission spectrum of 1-D oscillator chain without disorder

In order to use a 1-D oscillator chain as a filter, the oscillator at one end of the chain is excited, and the forced response vibration amplitude of the oscillator at the far end of the chain is measured. For the application of filtering a signal in an electrical circuit, a voltage can be used to drive the first resonator, and the vibration of the final resonator can be measured as a current, as shown in Fig. 3. The transmission of the filter can then be defined as the ratio of the power

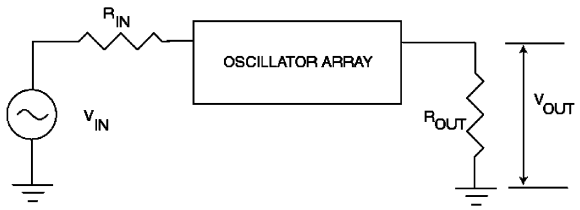

Fig. 3. Schematic of oscillator array in series with input and output impedances, R_{IN} and R_{OUT}. The force driving the first oscillator in the array is proportional to the voltage applied at the array input, while the current generated at the array output is proportional to the vibration amplitude of the final oscillator in the chain.

delivered into the load (output) impedance to the power delivered if the filter was replaced by a short circuit. The frequency spectrum of the transmission reveals the characteristics of the filter, as shown in Fig. 4. A high-quality filter has very low insertion loss and ripple, so that transmission is very nearly 1 within the passband, and low shape factor (ideally 1), so that transmission drops very sharply outside the passband.

As discussed in Section 2.1, the eigenvalues of the 1-D discrete Laplacian, given by $e(k) = 2/a^2(1 - \cos ka)$, are between 0 and $4/a^2$, corresponding to wavenumbers between 0 and π/a (wavelengths at least twice the spacing between oscillators). Since the corresponding frequencies are given by $\omega^2 = \omega_0^2(1 + e(k)a^2R)$, any frequency between ω_0 and $\omega_0\sqrt{1 + 4R}$ allows wave propagation along an infinite chain of oscillators. However, for a finite chain with N oscillators, there are N system resonances: N specific wavenumbers (within the range 0 to π/a) for which there is a match between the geometry of the wave and the geometry of the chain. These resonances can be found by assembling the equations of motion for all N oscillators into a matrix and solving for the system eigenvalues. The specific resonant frequencies, and the nature of the standing-wave resonant mode shapes, depend on the geometry of the chain as well as its end conditions. If the oscillator quality factor, Q, is sufficiently high, the frequency spectrum of the forced response of a finite oscillator array (and thus the transmission spectrum of the resulting filter) will feature distinct resonant peaks, one for each of the system resonances.

Fig. 5 shows the transmission spectrum for a filter comprised of five identical oscillators with Q of 10,000 and $R = 0.01$. Note that the frequency has been normalized as $(\omega/\omega_0 - 1)/2R$, so that the passband is nominally from 0 to 1. The curve is thus independent of oscillator frequency ω_0 or coupling R, and applies for any array for which $Q = 100/R$ (or $Q = 200Q_{\text{filter}}$). The five sharp peaks correspond to the five resonant frequencies of the coupled system. If this chain of oscillators were used in a filtering application, the result would be unacceptably high ripple within the passband. The resonant peaks can be flattened, however, by the proper use of termination resistors [6–8]. The input and output impedances, shown as R_{IN} and R_{OUT} in Fig. 3, are matched and adjusted to control the high Q of the system resonant peaks, thereby reducing passband ripple. These resistors affect each resonant peak by an amount proportional to the participation of the first and last resonators in the corresponding system mode shape, i.e., peaks corresponding to modes with little or no end-resonator motion will remain sharp, while peaks corresponding to modes with significant end-resonator motion will become much broader. Note that, although the termination resistors affect the overall shape factor of the filter (due to the broadening of the resonant peaks), their presence does not increase the filter insertion loss since

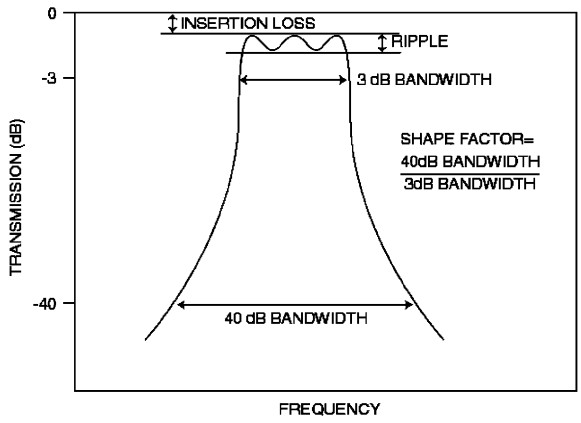

Fig. 4. Parameters for filter specification.

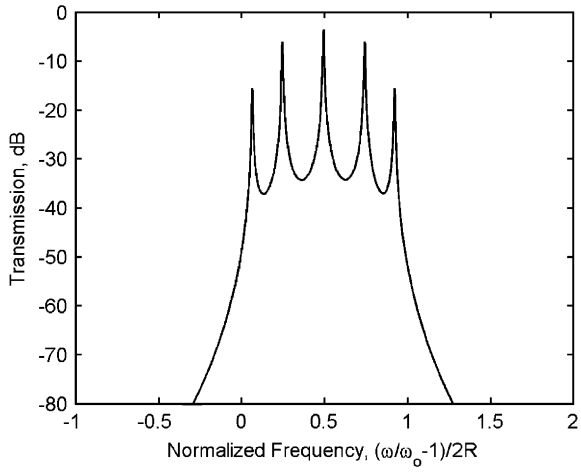

Fig. 5. Transmission spectrum of a 1-D chain of five identical high-Q oscillators.

they are external to the filter. For an array with identical resonators, the inherent dissipation in each resonator is the only source of loss present in the array but not present in the reference short circuit.

Fig. 6 shows the effect of increasing inherent oscillator damping (decreasing Q) for a 5-oscillator chain. As damping increases, the passband does not become distorted, but the increasing spatial decay of signals propagating across the chain results in greater insertion loss. To minimize insertion loss, oscillator Q must be large relative to Q_{filter} (δ/R must be small). For a filter with 2% bandwidth, $R = 0.01$ ($Q_{\text{filter}} = 50$), so insertion loss is less than 1 dB when $Q = 2500$, and damping effects are negligible for $Q = 100{,}000$. As bandwidth is decreased, however, Q_{filter} increases, resulting in greater loss unless the oscillator Q is also improved.

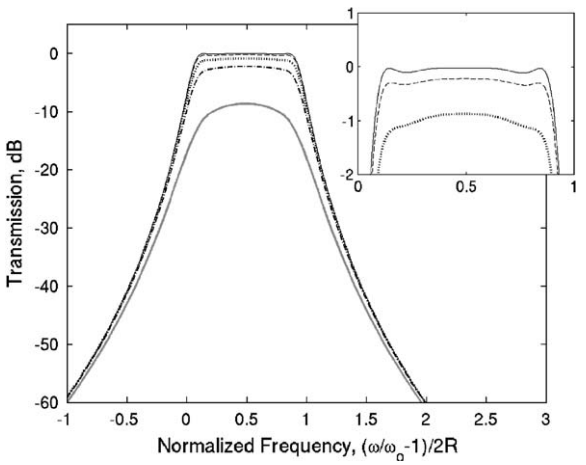

Fig. 6. Transmission spectra of ideal 1-D 5-oscillator chains with various oscillator quality factor Q: $Q = 2000Q_{\text{filter}}$ (—), $Q = 200Q_{\text{filter}}$ (- -), $Q = 50Q_{\text{filter}}$ (…), $Q = 20Q_{\text{filter}}$ (– ·), and $Q = 5Q_{\text{filter}}$ (-), corresponding to δ/R of 0.001, 0.01, 0.04, 0.1, and 0.4, respectively. The inset is a close-up of the passband.

3.2. Transmission spectra of disordered 1-D oscillator chains

The presence of disorder, like damping, results in spatial decay of signals propagating across the oscillator chain, but also in distortion of the passband due to changes in the resonant frequencies of the chain. As shown in Eqs. (12) and (13), the effect of disorder on the damped localization factor γ_{md} approaches the same level as the effect of dissipation as $(\sigma/R)^2$ approaches (δ/R). Once $(\sigma/R)^2$ is of greater order than (δ/R), increasing oscillator Q no longer decreases insertion loss, since disorder is the dominant cause of attenuation. Moreover, if $(\sigma/R)^2$ is not negligibly small, γ_{md} can become large enough that there are significant decreases in transmission within the passband, causing significant increases in both insertion loss and ripple, and hence degrading the filter performance. Narrow bandwidth applications require a coupling ratio, R, on the order of a few percent or even a few tenths of a percent. With current fabrication tolerances, it is not unreasonable to expect that the variation among resonators is of similar order. The contribution to spatial decay due to disorder ceases to be small as the ratio of disorder to coupling, σ/R, approaches 1.

The results of numerical simulations of three randomly disordered chains of five oscillators are shown: one with $\sigma/R = 0.2$, a second with $\sigma/R = 1$, and a third with $\sigma/R = 2$. In all cases, losses due to damping are negligible ($\delta/R = 10^{-3}$, or $Q = 2000Q_{\text{filter}}$). The results are shown in Fig. 7. For the first case, the transmission spectrum very nearly matches that of an ideal oscillator chain with no disorder: although greater than the effect of damping, the effect of disorder is still quite small. If disorder is of the same order as coupling ($\delta/R = 1$), its effects become more noticeable. Eq. (12) is no longer a valid approximation of spatial decay, even in the limit of large N, and distortion of the filter passband is evident, due to the changes in both the system natural frequencies and the corresponding mode shapes. The utility of the oscillator chain as a filter diminishes quickly as disorder is further increased. When $\sigma/R = 2$, the oscillator natural frequencies have random deviations on the same order as the width of the passband, and transmission loss is as high as 13 dB at some frequencies within the passband.

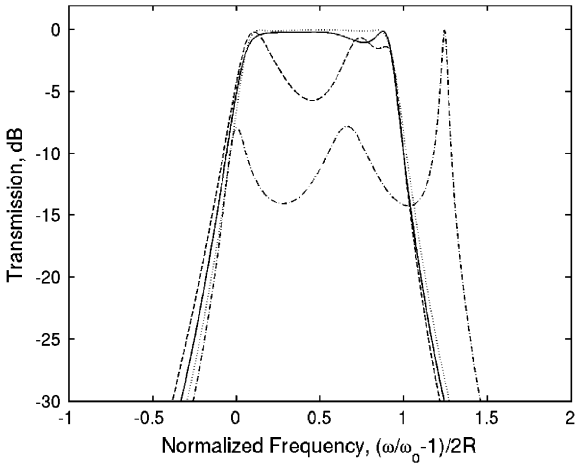

Fig. 7. Transmission spectra for 1-D 5-oscillator chains with varying levels of disorder. Each oscillator's stiffness varies from the nominal value by a random amount, selected from a population with standard deviation σ. The ideal case, $\sigma = 0$ (…), is shown along with three disordered cases: $\sigma = 0.2R$ (—), $\sigma = R$ (- -), and $\sigma = 2R$ (– ·), where R is the non-dimensional coupling.

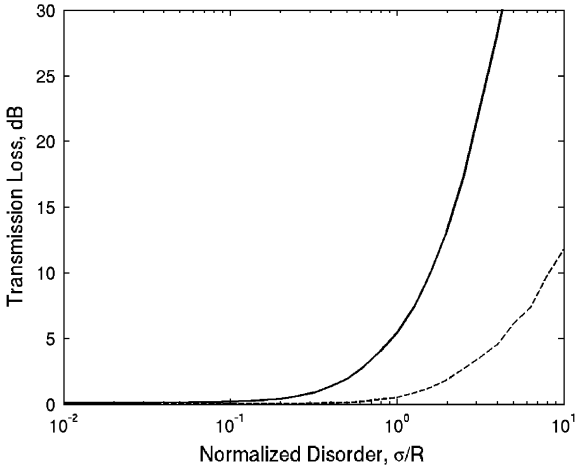

Fig. 8. Transmission loss within the passband as a function of normalized disorder for a 1-D oscillator array. "Maximum passband loss" (—) is the median value over 2000 random cases of the highest transmission loss within the passband, and "minimum passband loss" (- -) is the median value over 2000 random cases of the lowest transmission loss within the passband.

Note that the transmission spectra shown in Fig. 7 are for specific random cases, selected to illustrate typical results. Fig. 8 shows more general results based on a large number of simulations. At various levels of normalized disorder, σ/R, 2000 randomly disordered cases were simulated, and the highest and lowest transmission loss within the passband were calculated for each case, taking into consideration possible shifts in the passband center frequency. The median values of

these losses are plotted as a function of normalized disorder, demonstrating dramatic passband losses due to localization when disorder, σ, exceeds the coupling ratio, R.

4. Two-dimensional arrays

4.1. Reduction in sensitivity to disorder

As seen above, even small reductions in the amount of disorder can have a significant beneficial effect, since the coefficient of exponential decay governing spatial attenuation is a function of $(\sigma/R)^2$. However, the amount of disorder is typically determined by manufacturing tolerances, thus, disorder cannot be easily reduced without development of new manufacturing techniques with improved precision. Increasing the coupling between resonators, R, has the same effect as reducing disorder, yet this cannot be accomplished in a 1-D array without altering the filter bandwidth. A strongly coupled array is insensitive to disorder, yet narrow bandwidth applications dictate the use of weakly coupled arrays.

Consider a 2-D array of single-degree-of-freedom oscillators, weakly coupled in one direction, and strongly coupled in the other, as shown in Fig. 9. Note that both weak and strong coupling is to the same degree of freedom: this model represents an array in which a single mode of each resonator is coupled to the same mode in four adjacent resonators. Compared to the mechanical elements that couple the resonators in the weak direction, those in the strong direction must have different geometry and/or attachment locations closer to antinodes of the resonators, resulting in greater coupling stiffness. In an array with no disorder, the equation of motion for an oscillator with indices n and m, in the vertical and horizontal directions, respectively, is

$$\begin{aligned} &-\omega^2 m u_{n,m} + (k_0 + 2k_c^{\text{weak}} + 2k_c^{\text{strong}})u_{n,m} - k_c^{\text{weak}} u_{n-1,m} - k_c^{\text{weak}} u_{n+1,m} \\ &- k_c^{\text{strong}} u_{n,m-1} - k_c^{\text{strong}} u_{n,m+1} = 0. \end{aligned} \tag{14}$$

By noting that the terms involving coupling stiffnesses k_c^{weak} and k_c^{strong}can be grouped into a form resembling the 2-D discrete Laplacian, the similarity to the 2-D wave equation is apparent. Substituting $u_{n,m} = \exp(-\mathrm{i}\omega t)$, $u_{n-1,m} = \exp(-\mathrm{i}\omega t - \mathrm{i}k_w a_w)$, $u_{n,m-1} = \exp(-\mathrm{i}\omega t - \mathrm{i}k_s a_s)$, etc., where k_w and k_s are wavenumbers in the vertical (weakly coupled) and horizontal (strongly coupled) directions, and a_w and a_s are the oscillator spacings in those directions, the passband frequencies are found to be

$$\omega_2 = w_0 2(1 + 2(1 - \cos\, k_s a_s)R_s + 2(1 - \cos\, k_w a_w)R_w) \tag{15}$$

for the ideal array. Here, the coupling ratios R_w and R_s equal k_c^{weak}/k_0 and k_c^{strong}/k_0, respectively, so that $R_s > R_w$. As in the 1-D case, wavelengths shorter than twice the oscillator spacing cannot occur: any state with $k_s \geqslant \pi/a_s$ or $k_w \geqslant \pi/a_w$ is equivalent to a state with smaller wavenumber. Eq. (15) reveals the behavior of waves traveling along either of the two array directions: for any given wavenumber k_w in the vertical direction, there is a wide frequency band (with width governed by R_s) in which energy propagates in the horizontal direction, while for any given wavenumber k_s along the horizontal dimension, there is only a narrow band, defined by R_w, in which energy propagates vertically.

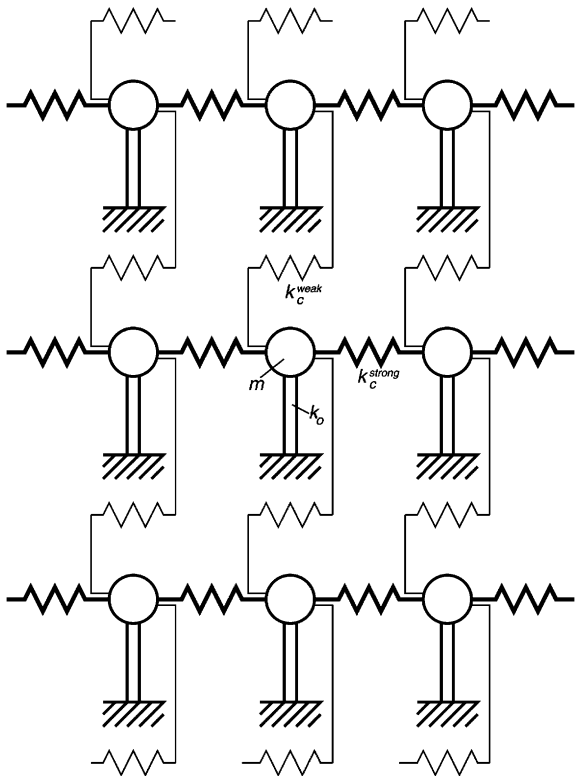

Fig. 9. Single degree of freedom model of a 2-D oscillator array. Each oscillator has the same mass, m, and nominal stiffness, k_0. Adjacent oscillators are coupled by stiffness k_c^{strong} in the horizontal direction and k_c^{weak} in the vertical direction.

Disorder is again modeled as variations in the stiffness of each oscillator from the nominal value, k_0, and characterized by σ, the standard deviation of those variations. The coupling in the weak direction, R_w, is chosen based on the desired bandwidth, even though this results in a non-negligible disorder-to-coupling ratio, σ/R_w. Meanwhile, the coupling in the other direction is chosen so that R_s is much greater, high enough that $(\sigma/R_s)^2$ is negligibly small. In this way, waves can propagate along each row of the array without significant attenuation, across a wide band of frequencies, but wave propagation along each column of the array is governed by the weaker coupling, allowing the desired narrow bandwidth.

The advantage of this configuration is that there are many pathways for energy to propagate in the weakly coupled direction, unlike the single pathway present in the 1-D array. In a 1-D array, as discussed in Section 2.3, the difference between one oscillator and the next causes a partial reflection of energy-carrying waves, resulting in spatial attenuation along the chain. In a 2-D array, each oscillator in a given row transmits energy, through the weak coupling, to its neighbor in the next row, and again, partial reflections result from the differences between oscillators. However, energy can also propagate *along* each row, and the strong coupling between oscillators in the same row ensures that the disorder within a row has little effect: disorder-induced spatial attenuation along each row is negligible. Because of this, each row can effectively act as a single

oscillator, and the total fraction of energy transmitted from one row to the next is the average of the transmission at each location where the two rows are coupled. If all oscillators in a given row vibrate with equal amplitude (as is the case if $|k_s| = 0$ or π/a_s), the transmission to the next row is thus governed by the difference between the *average* oscillator in the given row and the *average* oscillator in the next row. Since the disorder in oscillator stiffnesses is a random variable with standard deviation σ, the average stiffness of any N oscillators also varies randomly, but with standard deviation $\sigma/\sqrt{N}$ [35]. Thus, the greater the number of oscillators per row, the smaller the differences between each row's average stiffness. A 2-D array with N_w oscillators in the weak-coupling direction and N_s oscillators in the strong-coupling direction can thus act as an effective 1-D array with N_w oscillators and effective disorder $\sigma_{\text{eff}} = \sigma/\sqrt{N_s}$.

4.2. Resonant modes of a 2-D array and excitation of specific mode groups

Just as the resonant modes of a finite 1-D array are characterized by the number of wavelengths along the chain length, the modes of a 2-D array can be characterized by the number of wavelengths in each of the array directions. At resonance, standing-wave shapes will occur in each direction, and all oscillators in a given row will not necessarily have the same amplitude. In this more general case, transmission from one row to the next occurs most readily near antinodes of the standing wave shape in the strongly coupled direction. The total transmission between rows is thus governed not by a strict average of the stiffnesses of all oscillators in each row, but by a weighted average taking into account the modal participation of each oscillator. For example, at modes with standing wavelength in the strongly coupled direction equal to four times to oscillator spacing ($|k_s| = \pi/2a_s$), every even oscillator in the row will be at a node, and the odd oscillators will all have the same amplitude, albeit with alternating sign. In this case, the transmission between rows is governed by the difference among rows of the average of all *odd* oscillators in each row. Treating the 2-D array as an effective 1-D array, the effective disorder becomes $\sigma_{\text{eff}} = \sigma/\sqrt{N_s/2}$, for N_s even, or $\sigma_{\text{eff}} = \sigma/\sqrt{(N_s+1)/2}$, for N_s odd.

Fig. 10 shows the eigenvalues (the square of the natural frequencies) of a 5×7 array: five rows are weakly coupled to each other ($N_w = 5$), with each row containing seven oscillators strongly coupled to one another ($N_s = 7$). The resonances shown are for "fixed" boundary conditions, in which all exterior oscillators are coupled to rigid supports as well as to their nearest neighbors (for this boundary condition, resonance occurs for wavenumbers k such that $(N+1)ka/\pi$ is an integer). There are seven possible standing waves in the strongly coupled direction, and five in the weakly coupled direction—the 35 resonances are thus arranged in seven groups of five. The overall passband of the system, which consists of frequencies ω_0 to $\omega_0\sqrt{1+4R_s+4R_w}$, contains all 35 resonances. Within that band are seven sub-passbands that include five resonances each; the width of these is governed solely by R_w. Within each of these narrow passbands, the five resonant mode shapes all have the same wavenumber in the strongly coupled direction.

By forcing the oscillators in the first row in such a way as to excite only the modes with a certain strong-coupling-direction wavenumber, k_s, and measuring the vibration of the oscillators in the final row, the array can be used as a filter in the weak-coupling direction, with a single narrow passband selected by the wavenumber of the excitation applied to the first strongly coupled row. For example, resonances in the central passband (in the 5×7 array case, this is the fourth passband, consisting of resonances for which $k_s^* = 4$) all have wavelength in the strong-coupling

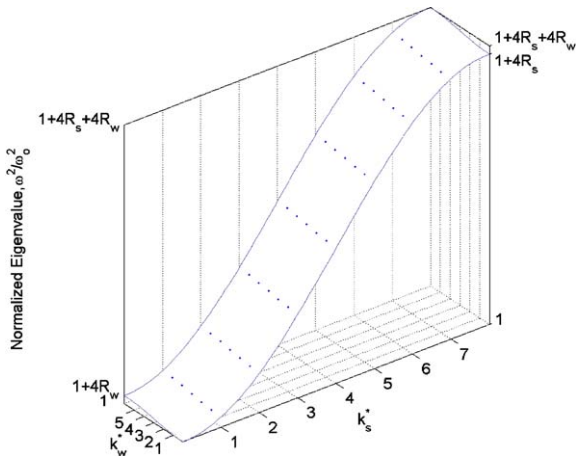

Fig. 10. Eigenvalues of a 5×7 2-D array of oscillators, plotted versus k_w^* and k_s^*, the normalized wavenumbers in the weakly and strongly coupled directions ($k_w^* = k_w a_w (N_w + 1)/\pi$, and $k_s^* = k_s a_s (N_s + 1)/\pi$). All 35 eigenvalues (represented by ●) lie on a surface defined by $1 + 2R_s(1 - \cos k_s a_s) + 2R_w(1 - \cos k_w a_w)$.

direction equal to four times the oscillator spacing a. The amplitude thus follows a pattern proportional to "1, 0, −1, 0, 1…" across each row. By exciting every odd oscillator in the first row, with phases alternating between 0° and 180°, this group of resonances can be selected, and the 2-D array acts as a filter with passband from $\omega_0\sqrt{1 + 2R_s}$ to $\omega_0\sqrt{1 + 2R_s + 4R_w}$. Thus, the width of the passband is governed by the weak-coupling ratio, R_w, while its center frequency is governed by the strong-coupling ratio, R_s, and by the choice of the mode-group excited. Note that, as in the 1-D case, proper selection of input and output impedances can smooth the ripple in the filter transmission spectrum caused by the five distinct resonances within the selected passband.

Excitation of a single wavenumber in the strongly coupled direction, resulting in the selection of a single narrow passband, is possible for an ideal array, with identical oscillators, due to the orthogonality of the mode shapes. However, the presence of disorder alters the modes of the system so that modes in other groups are not perfectly orthogonal to the excitation pattern. Since disorder entails, by definition, *small* variations among the oscillators, the modes in the desired group will be most strongly driven, as other modes will still be *nearly* orthogonal to the excitation. Fig. 11 compares the results of simulations of an ideal 5×7 array with those of a 5×7 array with disorder. The excitation is on the first row, with every odd oscillator driven, and alternating phase. For the ideal array, this excitation drives a response in the five resonances for which $k_s^* = 4$, but is orthogonal to all other modes, so a single passband is observed. In the disordered case, however, the vibration occurs in seven different passbands: a weak response is observed in six extraneous passbands in addition to the strong response in the desired passband.

As the number of oscillators in the strongly coupled direction is increased, the number of extraneous passbands increases, and, unless R_s is also increased to widen the overall frequency band, the passbands will become more closely spaced. Because the resonant frequencies are related to the cosine of the wavenumbers, the extra passbands are most closely spaced at the lowest and highest extremes. Exciting the central passband is thus an excellent choice, since it has the greatest separation in frequency from other, extraneous passbands. In addition, excitation of

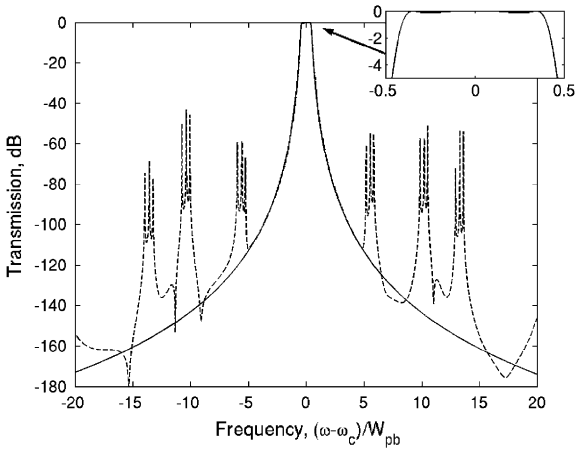

Fig. 11. Frequency spectrum of a 5×7 2-D array, driven to excite the central passband. The inset is a close-up of the passband (for the ideal case only) showing the removal of ripple by use of termination resistors. Ideal array (—), disordered array (- -).

this passband is relatively straightforward due to the fact that all oscillators that vibrate do so with the same amplitude.

4.3. Extra damping to suppress extraneous passbands

In addition to isolation in the frequency spectrum and ease of excitation, the choice of the central mode group for the filter passband presents one further advantage. In the central mode group, all odd oscillators in a given row are at *antinodes* of a standing wave in the strongly coupled direction, and thus vibrate with equal amplitude. Furthermore, all even oscillators are at *nodes* of the standing wave, and thus do not vibrate. However, all even oscillators are *not* at nodes for the other mode groups, in which the wavenumber in the strongly coupled direction is different. Adding damping to these even oscillators can thus suppress vibration in the other mode groups. Although this would not be necessary in an ideal case, in which there is no forcing of modes in any other groups, it can provide significant benefit in any real case, in which some disorder is present, and all other mode groups are excited (although at a reduced level). Fig. 12 shows the simulated frequency spectrum for a 5×7 array, in which the even numbered oscillators in each row have additional dissipation added so that damping coefficient δ (or $1/Q$) for these oscillators is significantly greater than the weak-coupling ratio R_w. By comparison with Fig. 11, it can be seen that the extra damping has suppressed any significant transmission in the extraneous passbands, but left the desired passband virtually unchanged.

4.4. Comparison of 1-D and 2-D arrays with disorder

As discussed in Section 4.1, a 2-D oscillator array, with strong coupling in one direction and weak coupling in the other, can act as an effective 1-D array, with each strongly coupled row of oscillators acting as a single effective oscillator with properties that are a weighted average of the

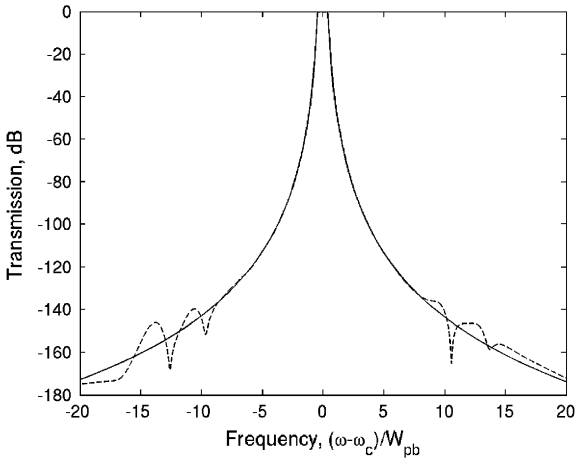

Fig. 12. Frequency spectrum of a 5×7 2-D array with extra damping on all oscillators in even columns, to suppress extraneous passbands. Ideal array (—), disordered array (- -).

properties of the oscillators in that row. If the excitation of the array is such that the central mode group is driven (i.e., standing waves are excited along the strong-coupling direction with wavelength equal to four times the oscillator spacing), then the weighted average is simply an average across all odd oscillators. The effective disorder (the standard deviation of the row averages) is less than the actual disorder (the standard deviation of the stiffnesses of individual oscillators) by a factor equal to the square-root of the number of odd oscillators in each row, which is $N_s/2$ if N_s is even, and $(N_s+1)/2$ if N_s is odd.

Fig. 13 shows close-ups of the passbands of simulated disordered 2-D arrays, each with five oscillators in the filter (weakly coupled) direction ($N_w = 5$), but with varying numbers of oscillators in the perpendicular (strongly coupled) direction (N_s is 1, 7, 17, or 49). Note that Fig. 13(a), for which $N_s = 1$, is actually the result of a 1-D array with five oscillators. In all cases, the inherent Q of each oscillator is high enough that damping-induced transmission losses (other than those due to intentionally added damping) can be neglected. In all 2-D cases, extraneous passbands, which lie outside the frequency range shown in the plots, are suppressed by the addition of damping to even oscillators, as described in Section 4.4.

For the 1-D case shown in Fig. 13(a), disorder, σ, equal to twice the weak-coupling ratio, R_w, is enough to cause significant distortion of the transmission spectrum. The passband is shifted somewhat in frequency, and strong ripple is present, with almost 20 dB transmission loss at some frequencies within the passband. This passband distortion is mitigated in the 2-D cases, Fig. 13(b)–(d): as N_s increases, the effective disorder decreases, so that the passband more closely resembles that of an ideal filter with no disorder. For $N_s = 49$, for which the effective stiffness of each row is an average of the stiffnesses of 25 different oscillators, the effective disorder is one-fifth the actual disorder, so that $\sigma_{\text{eff}}/R_w \approx 0.4$, and transmission spectrum distortion is dramatically reduced. Note that all cases shown in Fig. 13 are typical results: each is based on a single simulation, chosen so that the maximum transmission loss in the passband is near the median value of many simulations; i.e., half of all randomly disordered simulation cases have less transmission loss than the case shown, and half have more.

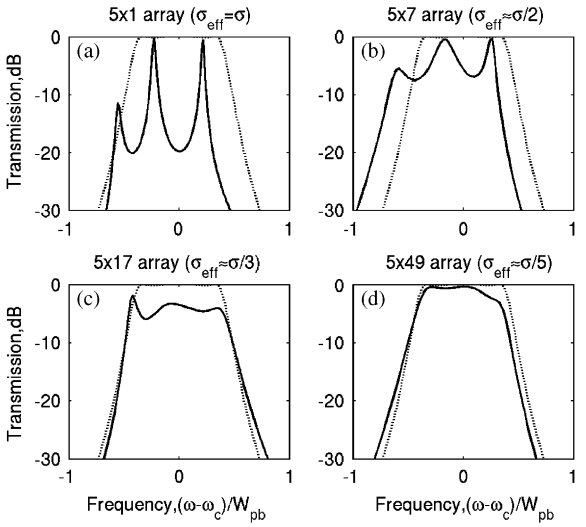

Fig. 13. Transmission spectra for various array sizes: (a) 5×1 array, (b) 5×7 array, (c) 5×17 array, and (d) 5×49 array. Ideal array (⋯), disordered array (—) (with standard deviation $\sigma = 2R_w$).

Increasing the number of oscillators in the strong-coupling direction, N_s, provides a benefit only if spatial decay in the strong-coupling direction remains negligible. Although σ/R_s is small (due to the high value of R_s), this quantity governs the average decay *per oscillator*. Thus, although localization does not occur over short distances, as in the weak-coupling direction, it can still occur in the strong-coupling direction if the length of each row is great enough. This effect is illustrated in Fig. 14. For a variety of array sizes, and for each of two strong-coupling ratios ($R_s = 15R_w$ and $R_s = 100R_w$), the highest transmission loss within the passband was determined for each of 5000 randomly disordered cases. The median value of this quantity is plotted against the "effective disorder" in the weak-coupling direction, i.e., the normalized disorder (σ/R_w) divided by the square root of the number of odd oscillators in each row. In all cases, the actual disorder σ is twice the weak-coupling ratio, R_w, thus, the disorder-to-coupling ratio in the strong-coupling direction is 0.13 and 0.02 for the two cases shown. For both cases, increasing N_s decreases the passband transmission loss as long as N_s is small. As N_s becomes large, however, localization in the strong-coupling direction becomes non-negligible, and further increases in N_s are no longer beneficial. This transition occurs at lower values of N_s for the $R_s = 15R_w$ case than for the $R_s = 100R_w$ case: for the latter, disorder has a smaller effect on transmission in the strong-coupling direction, so a larger number of oscillators per row is possible before localization in the strong-coupling direction becomes problematic.

As stated above, it is assumed here that dissipation-induced losses are small compared to disorder-induced losses, since it is in these situations that 2-D arrays provide the greatest benefit. Because the filter acts across the weak-coupling direction, dissipation-induced losses in a 2-D array are in general comparable to those in a 1-D array with the same value of resonator Q and a number of resonators equal to the number in the weak-coupling direction. This is true even for large numbers of resonators in each row (across the strong-coupling direction). However, dissipation-induced loss can place an upper limit on the useful number of resonators in each row.

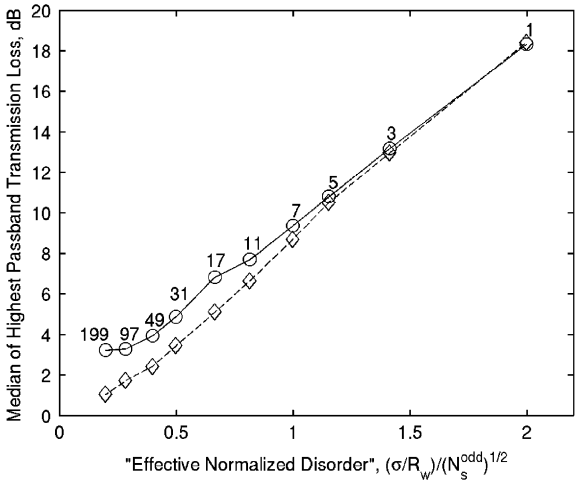

Fig. 14. Transmission loss within the passband as a function of array size for strong-coupling ratio $R_s = 15R_w$ (—) and $R_s = 100R_w$ (- -). "Highest Passband Transmission Loss" refers to the highest value of transmission loss within the passband of an individual randomly disordered case: the values plotted are the median values of 5000 cases for each array size. "Effective Normalized Disorder" is the normalized disorder, σ/R_w, divided by the square root of the number of odd oscillators per row. The number above each datum indicates the number of oscillators in the strong-coupling direction, N_s (the number of odd oscillators per row, N_s^{odd}, is thus $(N_s+1)/2$). For all cases, N_w is 5 and $\sigma/R_w = 2$.

In the same way that disorder-induced loss across each row becomes non-negligible when the number of resonators per row is sufficiently large, dissipation-induced loss can also become significant, and impede the ability of all oscillators in each row to cooperate as a single effective oscillator.

One final upper bound on practical values of N_s is imposed by the added complexity of fabricating arrays with very large numbers of resonators. The practicability of very large arrays, and thus the value of N_s at which the benefits of improved filter performance are outweighed by the increased fabrication difficulty, depends greatly on the fabrication technique. Note that, unlike macroscopic devices, microscale resonators have the advantage that the overall size of the array remains quite small even for large numbers of resonators, and thus, very large arrays are potentially feasible.

5. Conclusions

Due to their small size and low power requirements, arrays of micromechanical resonators show great promise for replacing the crystal and SAW resonators currently used as bandpass filters in communications devices. However, localization of vibration, due to unintended but unavoidable differences among resonators, can result in dramatic degradation of their filter characteristics. In particular, for 1-D arrays, localization is of significant concern when the amount of disorder approaches or exceeds the amount of inter-resonator coupling. Since the narrow bandwidth requirements of such devices dictate coupling as low as a tenth of a percent, even the small disorder due to manufacturing tolerances can result in localization. 2-D arrays,

strongly coupled in one direction and weakly coupled in the other, offer reduced sensitivity to variation among resonators, allowing high-order, narrow-bandpass filters to be implemented without the need for post-manufacture adjustment of individual resonators to compensate for disorder.

Acknowledgements

The authors gratefully acknowledge the financial support of the Office of Naval Research (ONR) and the Defense Advanced Research Projects Agency (DARPA). This research was performed while the first author held a National Research Council Research Associateship Award at the Naval Research Laboratory.

References

[1] C.T.-C. Nguyen, Micromechanical resonators for oscillators and filters, *Proceedings of the 1995 IEEE Ultrasonics Symposium*, Cannes, France 1 (1995) 489–499.
[2] C.T.-C. Nguyen, R.T. Howe, An integrated CMOS micromechanical resonator high-Q oscillator, *IEEE Journall of Solid-State Circuit* 34 (4) (1999) 440–445.
[3] C.T.-C. Nguyen, Frequency selective MEMS for miniaturized low-power communications devices, *IEEE Transactions on Microwave Theory and Techniques* 47 (8) (1999) 1486–1503.
[4] K. Wang, A.-C. Wong, C.T.-C. Nguyen, VHF free-free beam high-Q micromechanical resonators, *IEEE Journal of Microelectromechanical Systems* 9 (3) (2000) 347–360.
[5] L. Lin, R.T. Howe, A.P. Pisano, Microelectromechanical filters for signal processing, *IEEE Journal of Microelectromechanical Systems* 7 (3) (1998) 286–294.
[6] K. Wang, C.T.-C. Nguyen, High-order micromechanical electronic filters, *Proceeding of the 1997 IEEE International Workshop on Micro Electro Mechanical Systems*, Nagoya, Japan, January 1997, pp. 25–30.
[7] K. Wang, C.T.-C. Nguyen, High-order medium frequency micromechanical electronic filters, *IEEE Journal of Microelectromecanical Systems* 8 (4) (1999) 534–557.
[8] F.D. Bannon III, J.R. Clark, C.T.-C. Nguyen, High-Q HF micromechanical filters, *IEEE Journal of Solid-State Circuits* 35 (4) (2000) 512–526.
[9] B.H. Houston, D.M. Photiadis, J.F. Vignola, M.H. Marcus, X. Liu, D. Czaplewski, L. Sekaric, J. Butler, P. Pehrsson, J.A. Bucaro, Loss due to transverse thermoelastic currents in microscale oscillators, *Materials Science and Engineering A* 370 (2004) 407–411.
[10] L. Brillouin, *Wave Propagation in Periodic Structures*, second ed, Dover Publications, New York, 1953.
[11] D.J. Mead, Wave propagation and natural modes in periodic systems, I: mono-coupled systems, *Journal of Sound and Vibration* 40 (1975) 1–18.
[12] P.W. Anderson, Absence of diffusion in certain random lattices, *Physical Review* 109 (1958) 1492–1505.
[13] C.H. Hodges, Confinement of vibration by structural irregularity, *Journal of Sound and Vibration* 82 (1982) 411–424.
[14] P.J. Cornwell, O.O. Bendiksen, Localization of vibrations in large space structures, *AIAA Journal* 27 (2) (1987) 219–226.
[15] C. Pierre, D.M. Tang, E.H. Dowell, Localized vibrations of disordered multi-span beams: theory and experiment, *AIAA Journal* 25 (1987) 1249–1257.
[16] S.D. Lust, P.P. Friedmann, O.O. Bendiksen, Mode localization in multi-span beams, *AIAA Journal* 28 (1990) 225–235.

[17] S.D. Lust, P.P. Friedmann, O.O. Bendiksen, Free and forced response of nearly periodic multi-span beams and multi-bay trusses, *Proceedings of the 32nd AIAA/ASME/ASCE/AHS/ASC Structures, Structural. Dynamics, and Materials Conference*, Baltimore, MD, 1991, pp. 2831–2842.
[18] D. Bouzit, C. Pierre, Vibration confinement phenomena in disordered, mono-coupled, multi-span beams, *Journal of Vibration and Acoustics* 114 (4) (1992) 521–530.
[19] D.M. Photiadis, E.G. Williams, B.H. Houston, Wave-number space response of a near periodically ribbed shell, *Journal of the Acoustical Society of America* 101 (2) (1997) 877–886.
[20] D.M. Photiadis, B.H. Houston, Anderson localization of vibration on a framed cylindrical shell, *Journal of the Acoustical Society of America* 106 (3) (1999) 1377–1391.
[21] M.B. Levine-West, M.A. Salama, Mode localization experiments on a ribbed antenna, *Proceedings of the 33rd AIAA/ASME/ASCE/AHS/ASC Structures, Structural Dynamics, and Materials Conference*, Dallas, TX, 1992, pp. 2038–2047.
[22] S.T. Wei, C. Pierre, Localization phenomena in mistuned assemblies with cyclic symmetry, part I: free vibrations, *Journal of Vibration, Acoustics, Stress, and Reliability in Design* 110 (1988) 429–438.
[23] S.T. Wei, C. Pierre, Localization phenomena in mistuned assemblies with cyclic symmetry, part II: forced vibrations, *Journal of Vibration, Acoustics, Stress, and Reliability in Design* 110 (1988) 439–449.
[24] M.P. Castanier, C. Pierre, Individual and interactive mechanisms for localization and dissipation in a mono-coupled nearly periodic structure, *Journal of Sound and Vibration* 163 (3) (1993) 479–505.
[25] P. Sheng, *Introduction to Wave Scattering, Localization, and Mesoscopic Phenomena*, Academic Press, San Diego, 1995 pp. 26-31 and 203-205.
[26] J.A. Bucaro, B.H. Houston, D.M. Photiadis, A.J. Romano, A. Sarkissian, X. Liu, S. Morse, J. Vignola, E.G. Williams, M. Marcus, L. Sekaric, Moving vibrational measurement techniques, methodologies, and concepts from macroscopic applications to the microworld, *Proceedings of the 2000 IEEE Ultrasonics Symposium*, San Juan, Puerto Rico 1 (2000) 513–524.
[27] X. Liu, S.F. Morse, J.F. Vignola, D.M. Photiadis, A. Sarkissian, M.H. Marcus, B.H. Houston, On the modes and loss mechanisms of a high Q mechanical oscillator, *Applied Physics Letters* 78 (10) (2001) 1346–1348.
[28] B.H. Houston, D.M. Photiadis, M.H. Marcus, Xiao Liu, J.A. Bucaro, Thermoelastic loss in microscale oscillators, *Applied Physics Letters* 80 (7) (2002) 1300–1302.
[29] D.M. Photiadis, B.H. Houston, X. Liu, J.A. Bucaro, M.H. Marcus, Thermoelastic loss observed in a high Q mechanical oscillator, *Physica B* 316–317 (2002) 408–410.
[30] P. Mohanty, D.A. Harrington, K.L. Ekinci, Y.T. Yang, M.J. Murphy, M.L. Roukes, Intrinsic dissipation in high-frequency micromechanical resonators, *Physical Review B* 66 (8) (2002) 085416.
[31] D.M. Photiadis, J.A. Judge, Attachment losses of high Q oscillators, *Applied Physics Letters* 85 (3) (2004) 482–484.
[32] C.A. Bolle, V. Aksyuk, F. Pardo, P.L. Gammel, E. Zeldov, E. Bucher, R. Boie, D.J. Bishop, D.R. Nelson, Observation of mesoscopic vortex physics using micromechanical oscillators, *Nature* 399 (1999) 43–46.
[33] J. Yang, T. Ono, M. Esashi, Surface effects and high quality factors in ultrathin single-crystal silicon cantilevers, *Applied Physics Letters* 77 (23) (2000) 3860–3862.
[34] J. Yang, T. Ono, M. Esashi, Investigation surface stress: surface loss in ultrathin single-crystal silicon wafers, *Journal of Vacuum Science and Technology B* 19 (2) (2001) 551–556.
[35] J.S. Bendat, A.G. Piersol, *Random Data: Analysis and Measurement Procedures*, third ed, Wiley, New York, 2000 pp. 93–94.